

# Intermittent Slip along the Alto Tiberina Low-angle Normal Fault in Central Italy - Supporting Information

A. Vuan<sup>1</sup>, P. Brondi<sup>1</sup>, M. Sukan<sup>1</sup>, L. Chiaraluce<sup>2</sup>, R. Di Stefano<sup>2</sup>, M. Michele<sup>2</sup>

<sup>1</sup>National Institute of Oceanography and Applied Geophysics - OGS

<sup>2</sup>National Institute of Geophysics and Volcanology - INGV

## Contents of this file

Text S1 to S2

Figures S1 to S6

## Introduction

This supplementary information contains additional details on the template matching approach (Text S1) and declustering (Text S2). We also include info on the completeness magnitude (Figure S1), examples of matching detections (Figure S2), declustering operated in time and space (Figure S3), spatiotemporal along-strike projection of clustered and background seismicity on ATF (Figure S4), examples of cluster types (Figure S5) and comparative analysis of cumulative moment release on HW and ATF (Figure S6).

## Text S1 - Template Matching

In template matching, waveforms of previously identified earthquakes are used to discover similar events or quasi-repeaters by correlation with continuous data chunks. A network function is retrieved by shifting the single-channel cross-correlations for the event travel-time offset and by stacking. Applying a trigger threshold on the resulting stacked function, generally  $N$  times above the median absolute deviation (MAD), it is possible to retrieve low-magnitude earthquakes usually hidden below the noise level. This technique is capable of augmenting the number of detected earthquakes by a factor 5-10 (e.g., Shelly et al., 2007; Kato et al., 2012).

In the recent past, we optimized a template matching suite of codes named PyMPA, to run the demanding calculations for years of continuous waveforms and thousands of templates (Vuan et al., 2018). The code was applied in the 2009 L'Aquila, 2012 Emilia, and 2016 Central Italy seismic sequences (Sukan et al., 2014; Vuan et al., 2018; Sukan et al., 2019). PyMPA is applied in this study to daily three-component continuous waveforms covering the 2010-2014-time window, resampled at 25 Hz. Templates are trimmed using a 5s data window, starting 2.5 s before the theoretical S wave arrival, computed using the ObsPy port (Krisher et al., 2015) of the Java TauP Toolkit routines (Crotwell et al., 1999) and a suitable 1D-model (Latorre et al., 2016). We adopt Kurtosis-based tests to evaluate the signal-to-noise ratio of templates (Baillard et al., 2014) avoiding the use of unwanted signals in the matching technique (Vuan et al., 2018).

Seismic data from 2010 to 2014 are collected for 60 stations of the TABOO seismic network (Figure 1 in the manuscript; (Chiaraluce et al., 2014b) located within a radius of about 50 km from the investigated fault. The correlograms are evaluated as a function of time, shifting sample by sample the template event window through 4-hours chunks

---

Corresponding author: Alessandro Vuan, [avuan@inogs.it](mailto:avuan@inogs.it)

of continuous waveforms. The threshold, defined after a visual inspection of some examples of detected events, is set at nine times the MAD of the stacked correlograms. At each station, the magnitude of the detected event is estimated by comparing its amplitude with the template' amplitude, assuming that a tenfold increase in ratio corresponds to a one-unit increase in magnitude. Time windows of 5 s are selected, and within each one, the template, for which the normalized correlation coefficient is the greatest, is taken for determining the event location and magnitude (e.g., Kato et al., 2012).

We apply a bandpass filtering by selecting different frequency ranges. Calculation times can be reduced by subsampling the signals and using relatively low-frequency bands, even if the involved magnitudes are small. Therefore, we test several frequency ranges and find that waveforms resampled at 25 Hz and filtered between 3 and 8 Hz (Figures S2a, and S2b), even for small magnitudes, proves useful for the detection of events, saving considerable calculation time. Obviously, by using signals sampled at 100 Hz and filtering between 5 and 15 Hz (Figures S2c, S2d), the values that exceed the detection threshold (9 times the MAD) are higher. However, the cross-correlation values for each channel in most cases do not vary significantly as the estimated magnitude.

Low-pass templates can detect small events propagating at lower rupture velocity than regular earthquakes and having low static stress drop on a creeping fault, behaving similarly to low-frequency earthquakes (e.g., Kwiatek Ben-Zion, 2016).

In declaring a detection, we use very restrictive criteria as a) the stacked cross-correlation function threshold set at 9 times the MAD, b) the 12 channels that are the closest to the template location, and c) the cross-correlation mean values higher than 0.35. We also check by visual inspection the detections at lower threshold values and different frequency ranges and find that the average number of false detections is of about 5%, in the threshold range from 9 to 12 times the MAD.

The template matching method, similarly to Zhang and Wen (2015), usually relocates events around the position of the template. This relocation is made possible by the fact that for each channel the maximum value of the stacked cross-correlation function is determined within a limited time interval; here we use six samples shift at each channel (0.24 s at 25 Hz), lower than the 0.3 s single-channel residual in the location of templates. Therefore, we can move the position of the new detected event relative to the early arrivals or delays measured to achieve a maximized value of the stacking of all the cross-correlation functions. For each event with at least 12 recording channels, we construct a two-step 3D mesh with 500 and 100 m, respectively, centred at the position of the template. Then, we least-square minimize the residuals between the calculated travel-time at each grid point and the time shifts resulting from the single-channel cross-correlation. The mesh step and resolution of the relocation depend on the signal sampling rate; at 25 Hz, the location resolution varies between 500 and 1,000 m. Using this refined relocation, we then discarded the events that do not fall within 1 km from the supposed ATF plane as defined by the isobaths shown in Figure 1.

## Text S2 - Declustering

A statistical analysis of the ATF-Z+ catalogue is performed by a nearest-neighbour approach (Zaliapin Ben-Zion, 2016) to separate the background seismicity from the clusters. The nearest-neighbour method computes the time-space distance  $\eta$  between pairs of earthquakes. Rescaled time (T) and distance (R) between an event  $i$  and its parent  $j$  are normalized by the magnitude of  $j$  and expressed as:

$$T_{ij} = t_{ij} 10^{-pbm_i/2}; R_{ij} = r_{ij}^d 10^{-(1-p)m_i/2} \quad (1)$$

where  $p$  is a weight parameter,  $b$  is the Gutenberg-Richter  $b$ -value,  $m$  the magnitude of the  $i$  event,  $t$  and  $r$  are the time and distance between the two earthquakes, re-

90 spectively, and  $d$  is the fractal dimension. We fixed  $p = 0.5$ ,  $b=0$  (Zaliapin and Ben-Zion  
 91 (2020) justifies to use  $b = 0$  for small events) and  $d=1.6$ . Thus,  $\eta$ , the generalized dis-  
 92 tance between pairs of earthquakes, is formulated as:

$$93 \quad \log \eta_{ij} = \log R_{ij} + \log T_{ij} \quad (2)$$

94 **Figures S1 - S6**

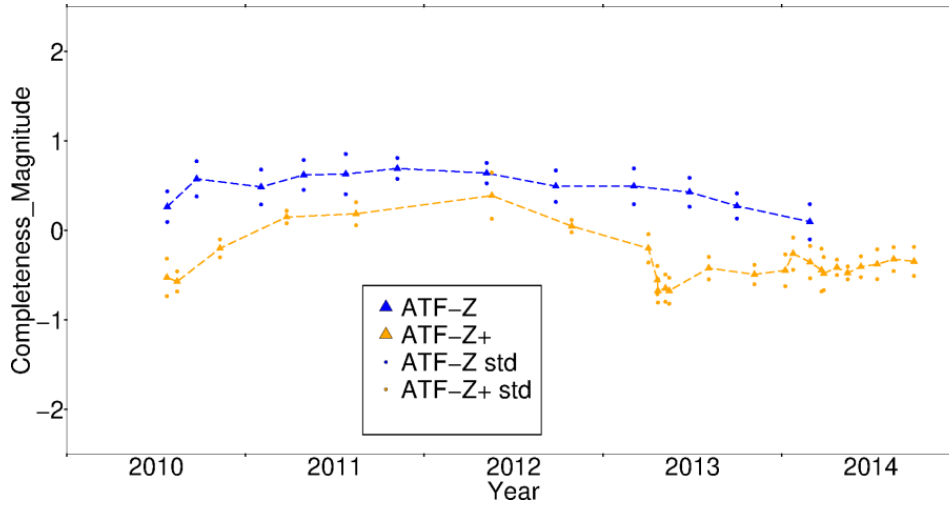


**Figure S1.** Time-dependent completeness magnitude ( $M_c$ ) for the ATF-Z catalogue (blue, templates), and the ATF-Z+ new catalogue (orange). The completeness magnitude is estimated using the b-value stability from Cao & Gao, 2002.

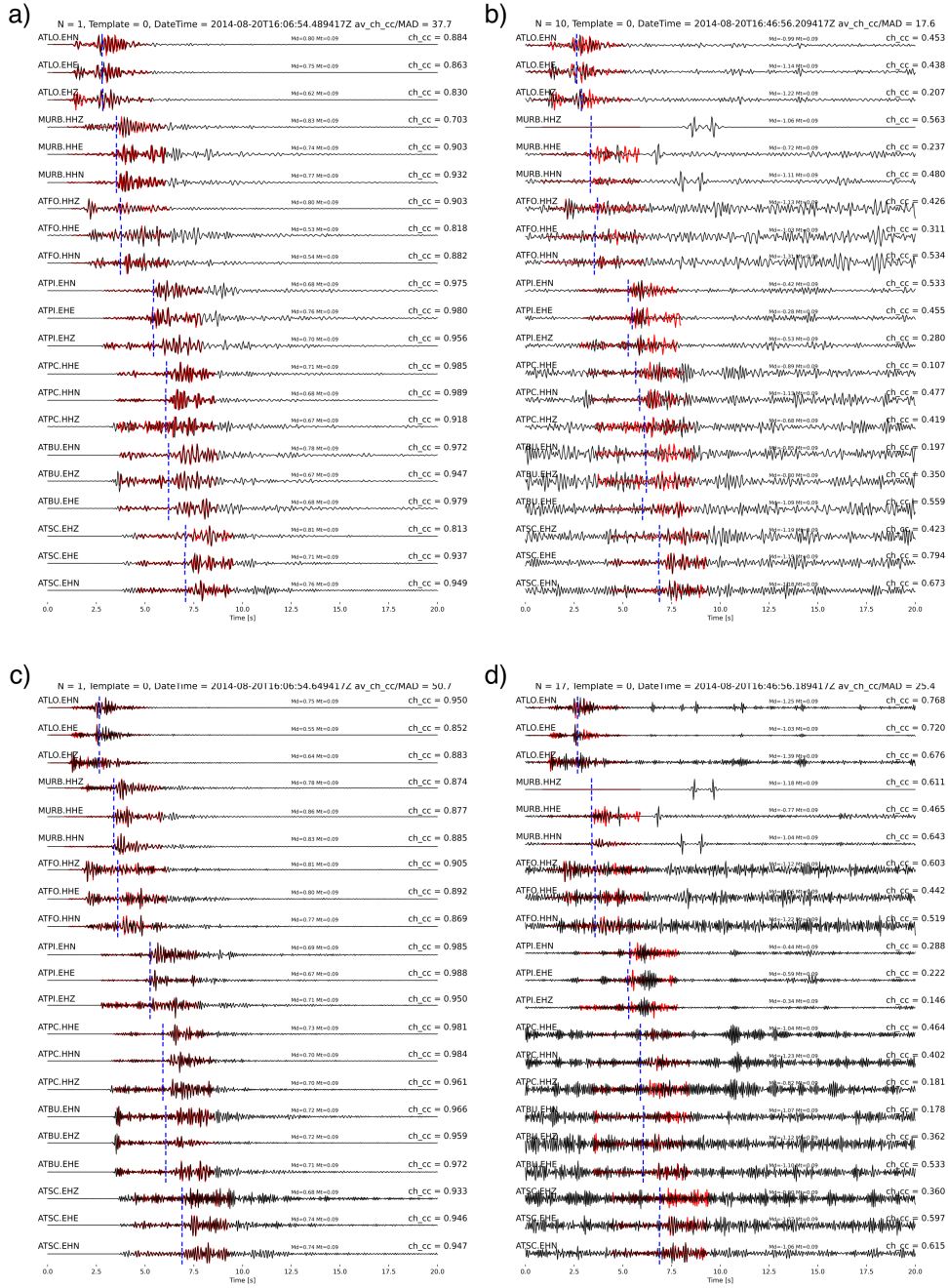


**Figure S2.** Examples of matching detections of an  $M_L=0.8$ , and  $M_L=-1$  events using the same  $M_L=0.0$  template on the ATF. a)  $M_L=0.8$  detection with template bandpass filtered between 3 and 8 Hz, (b)  $M_L=-1$  detection bandpass filtered between 3 and 8 Hz, c)  $M_L=0.8$  detection bandpass filtered between 5 and 15 Hz, d)  $M_L=-1$  detection bandpass filtered between 5 and 15 Hz.

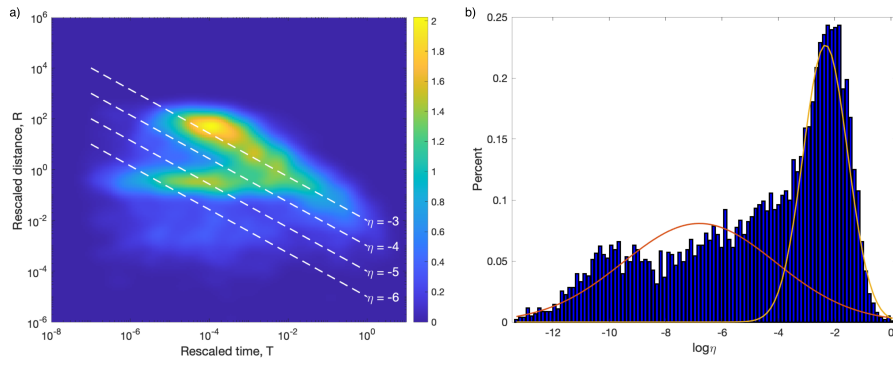


**Figure S3.** a) 2d rescaled T and R distances for the ATF augmented catalog. The distribution is bimodal and clusters are separated by using  $\eta = -4$ . b) histograms showing the distribution of the events and the selection of  $\eta = -4$  to decluster.

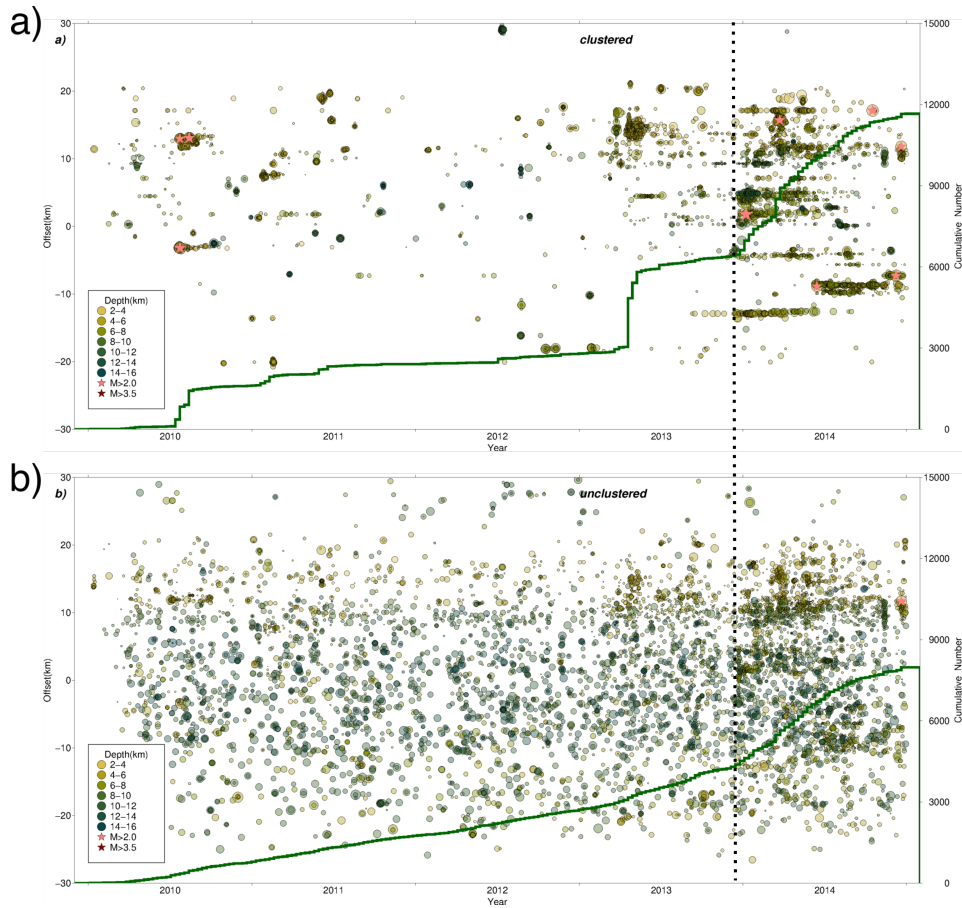


**Figure S4.** a) 2010-2014 spatiotemporal along-strike projection of clustered events on ATF and b) background seismicity (clusters with less than 10 events). Green line is showing the cumulative number of earthquakes in the selected catalogues. The dotted vertical line corresponds to the time of increased clusters and background seismicity in a 30 km long segment of the ATF.

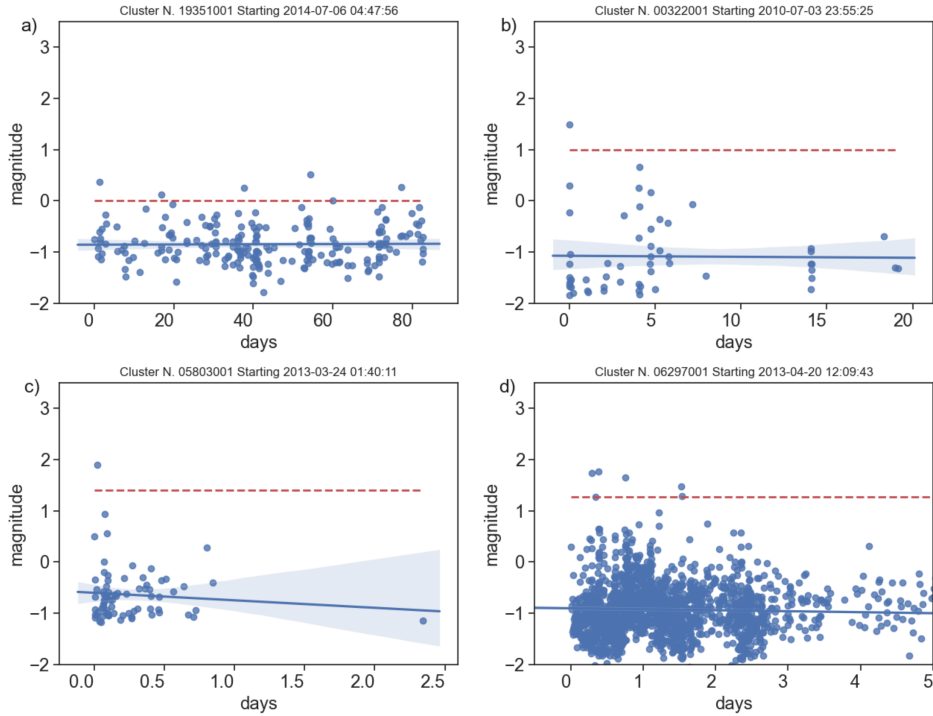


**Figure S5.** a) Swarm cluster, b) mainshock-aftershock cluster, and c) foreshock-mainshock, d) productive swarm clustered in time. The red dashed line indicates the 0.5 threshold below the largest magnitude event in a cluster while the blue solid line represents a linear regression of the cloud. Long duration swarms last up to 90 days but for some specific cases we found hundreds of clustered events within 3 – 5 days.

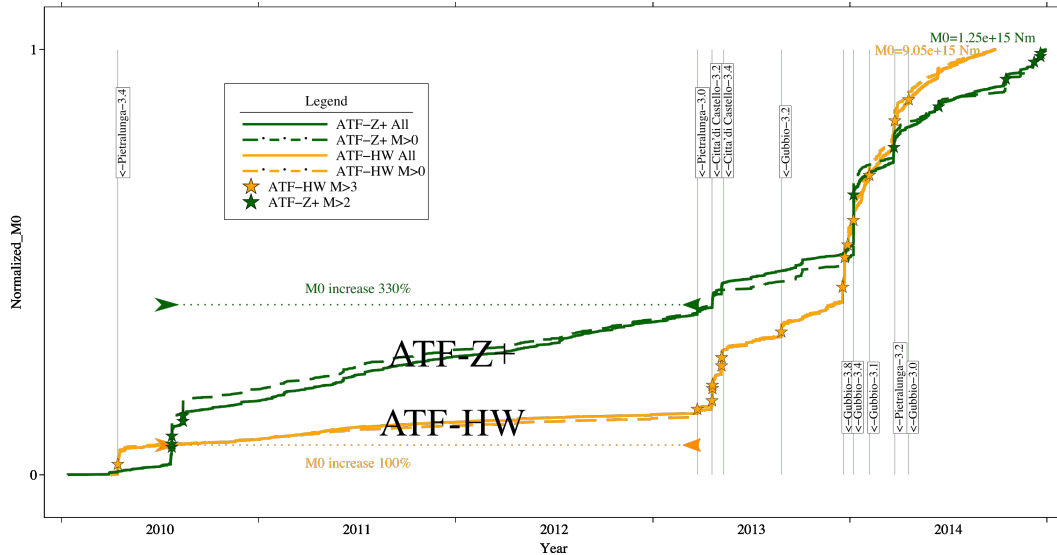


**Figure S6.** Normalized cumulative seismic moment for the ATF-HW and ATF-Z+ catalogues considering all the events (solid lines) and only  $M_L > 0$  (dashed). The ATF-HW cumulative moment is larger than that in ATF-Z+ within the 5-years. The difference in terms of seismic moment between the two catalogues varies from a factor of 2 (2010) to 7 (end of 2014). In the period where significant sequences are absent (dotted), the percentage moment growth is 3 times higher in the ATF-Z+ than in ATF-HW catalogue.